

Design of reinforced ground embankments used for rockfall protection

C. Ronco, C. Oggeri, and D. Peila

Dept. of Land, Environment and Geo-technology, Politecnico di Torino, Torino, Italy

Received: 3 February 2009 – Revised: 25 June 2009 – Accepted: 7 July 2009 – Published: 17 July 2009

Abstract. The prediction of the effects of rockfall on passive protection structures, such as reinforced ground embankments, is a very complex task and, for this reason, both full-scale tests and numerical dynamic modelling are essential.

A systematic set of numerical FEM models, developed in the dynamic field, has been implemented in this work to evaluate the conditions of an embankment that has been subjected to the impact of rock blocks of various sizes at different speeds. These analyses have permitted design charts to be obtained. Furthermore, a simplified analytical approach, based on an equilibrium analysis, has been proposed and its results are compared with numerical data in order to assess its feasibility. A good correspondence between the results has been obtained.

1 Introduction

Rockfall protection embankments are widely used to stop high kinetic energy rockfall events (Fig. 1), both in civil and in mining applications, in order to protect roads, inhabited areas, quarry plants or yards. Different embankment types (Table 1) made of natural compacted soil, huge rock blocks, gabions or reinforced ground have been used (Peckover and Kerr, 1977; Giani, 1992; Wyllie and Norrish, 1996; Oggeri and Peila, 2000; Nomura et al., 2002; Peila et al., 2007). The most frequent examples are reinforced embankments.

Despite the large number of installations, a design procedure has not been set up yet, because of problems related to the non linear stress-strain behaviour of the soil, the

large deformations that occur during impact and uncertainties regarding the dynamic behaviour of the soil and the soil-reinforcement interaction.

In order to understand the behaviour of ground reinforced embankments during impact, some full-scale tests have been carried out by various authors (Barrett and White, 1991; Burroughs et al., 1993; Peila et al., 1999, 2007; Tissieres, 1999; Yoshida, 1999). These experiments only permitted a limited number of variations of both the geometries and impact energies to be studied, due to their complexity. Furthermore, the numerical modelling developed to study ground reinforced embankments (Carotti et al., 2000; Castiglia, 2000; Di Prisco and Vecchiotti, 2003, 2006; Bertrand et al., 2005; Bertrand, 2006; Lambert et al., 2007, 2008; Peila et al., 2007; Plassiard et al., 2008) has generally been limited to the back-analysis of full-scale tests and these researches have not provided a general design procedure for this type of protection work.

Engineers, instead, need to have a simple design procedure that can provide a feasible and robust evaluation of the type and size of the structure that has to be used to withstand the impact energy of the forecasted rockfall and to quantify its safety factor.

In order to develop a general design scheme, based on evidence already acquired and reported in literature from full-scale tests, a systematic series of numerical models has been carried out to provide design guidelines that can help engineers choose embankment characteristics.

2 Full-scale tests on embankments

Full-scale tests have been carried out on prototype embankments by the Colorado Department of Transportation (Barrett and White, 1991); Burroughs et al. (1993); Protec Engineering (Yoshida, 1999; www.proteng.co.jp); Gifu University (Japan) (www.proteng.co.jp); Tissieres (1999) and by the



Correspondence to: C. Ronco
(chiara.ronco@polito.it)



Fig. 1. Example of rock elements stopped by a reinforced embankment (Aosta Valley, Italy) (courtesy Officine Maccaferri S.p.A.).

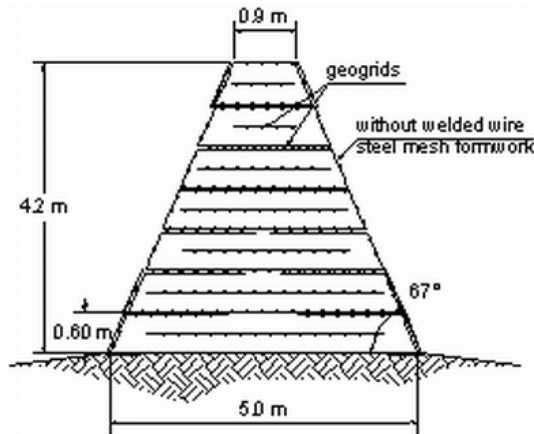




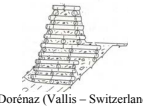
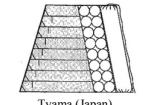



Fig. 2. Schematic cross section of the tested embankments (Peila et al., 2007).

Politecnico di Torino (Italy) (Peila et al., 1999, 2007). The latter research involved a complete series of tests on embankments made of sand and gravel reinforced with polymeric geogrids that was carried out using a cable device that is able to launch reinforced concrete blocks with a variable mass and a speed (measured at the impact time) of about 30 m/s and which is also used to study net fences (Peila et al., 1998; Peila and Oggeri, 2006). The obtained results made it possible to note that strata reinforced embankments mainly react through sliding on the surfaces that are defined by the geogrids during the impact by the block and that only a limited portion of the whole structure (near the impact point) directly bears the forces induced by the impact. Therefore, the block energy is dissipated in the frictional work, due to the sliding on the reinforcing elements, and in the plasticization of the soil directly involved in the impact, with the creation of a hole. The results obtained in these tests (Table 2) have been described in more detail (Peila et al., 1999, 2000, 2002, 2007).

In tests 1 and 2, the embankments were reinforced with polymeric mono-oriented geogrids, while in test 3 the embankment was left unreinforced. The dip of the faces was kept the same on both sides ($\approx 67^\circ$) with an upper layer thickness of 0.90 m (the smallest that could be obtained from a

Table 1. Embankment types and their constructive characteristics.

| Type | Geometry | Example | Reference |
|--|--|---|--|
| Embankment made of compacted soil | Isosceles trapezium Faces dip $\approx 35^\circ$ (with reference to horizontal) Usual max. height $\approx 5\text{--}6$ m |  Rasa quarry (Varese – Italy) | Paronuzzi (1989) Del Greco et al. (1994) |
| Embankment made up of huge rock blocks | Isosceles trapezium Faces dip $\approx 35^\circ$ (with reference to horizontal) Usual max. height ≈ 12 m |  Chatillon (Aosta Valley – Italy) | Pasqualotto et al. (2004) |
| Embankment made of compacted soil with one side made of gabions | Right-angle trapezium Valley-side face dip $\approx 35^\circ$ (with reference to horizontal) Mountain-side face dip $\approx 90^\circ$ (with reference to horizontal) |  Paluzza (Udine – Italy) | Oggeri et al. (2004) Lambert et al. (2008) |
| Embankment made of gabions | Isosceles trapezium or parallelepiped Valley-side face dip $70^\circ\text{--}90^\circ$ (with reference to horizontal) Mountain-side face dip $70^\circ\text{--}90^\circ$ (with reference to horizontal) |  (France) | Wyllie and Norrish (1996) Lambert et al. (2007) |
| Embankment made of compacted soil reinforced with wood and steel bars | Isosceles trapezium Faces dip $\approx 60^\circ\text{--}70^\circ$ (with reference to horizontal) |  Dorénaz (Vallis – Switzerland) | Tissières (1999) |
| Embankment made of reinforced ground with geotextiles or geogrids and with an adsorbing mattress | Isosceles trapezium Valley-side face dip $70^\circ\text{--}90^\circ$ (with reference to horizontal) Mountain-side face dip $70^\circ\text{--}90^\circ$ (with reference to horizontal) covered by big bags filled with sand (adsorbing mattress) |  Tyama (Japan) | Yoshida (1999) www.proteng.co.jp |
| Embankment made of reinforced ground with geotextiles, geogrids or metallic wire mesh | Isosceles trapezium Valley-side face dip $70^\circ\text{--}90^\circ$ (with reference to horizontal) Mountain-side face dip $70^\circ\text{--}90^\circ$ (with reference to horizontal) |  Rhemes Saint – Georges (Aosta Valley – Italy) | Lazzari et al. (1996) Burroughs et al. (1993) Peila et al. (2007) Pasqualotto et al. (2005) |

technological point of view), in order to test an embankment with the smallest cross-section that can be built (Fig. 2).

In test 1, the block, which had an energy of 2500 kJ, neither crossed nor damaged the embankment to any great extent: the crater on the mountain-side face had a maximum depth of 0.60 m and the extrusion of the soil layers on the valley-side was only about 0.17 m (Table 3). Furthermore, no significant deformation was observed outside the area directly affected by the impact. During test 2, the embankment was subjected to three impacts, which were repeated in the same position, at an energy of 4500 kJ, until the embankment collapsed. It was observed that, during the first and the second impacts (Fig. 3), the embankment successfully stopped the block and remained stable in spite of the large displacements of the soil layers that were observed after the second impact. After the third impact, the displacement on the valley-side face was very large and did not allow the stability of the structure to be maintained.

Test 3 was carried out on an unreinforced embankment, with the same geometry as in tests 1 and 2. The rock block was stopped, but the embankment collapsed after the impact (Fig. 4) due to a longitudinal tension crack that developed in

Table 2. Summary of the performed tests.

| Test number | Block mass [kg] | Impact energy [kJ] | Number of impacts | Soil | Maximum geogrid tensile strength [kN/m] |
|-------------|-----------------|--------------------|-------------------|---|---|
| 1 | 5000 | 2500 | 1 | Sand and gravel $c'=9$ kPa ; $\phi'=34^\circ$; $\gamma'=21.10$ kN/m ³ | 50 |
| 2 | 8700 | 4500 | 3 | Sand and gravel $c'=9$ kPa ; $\phi'=34^\circ$; $\gamma'=21.10$ kN/m ³ | 45 |
| 3 | 8700 | 4500 | 1 | Sand and gravel $c'=9$ kPa ; $\phi'=34^\circ$; $\gamma'=21.10$ kN/m ³ | Absent |

**Fig. 3.** Reinforced embankment after the second impact in test 2 (Peila et al., 2007).**Fig. 4.** Unreinforced embankment after the impact in test 3 (Peila et al., 2007).

the middle of the upper layer, along the embankment axis, while the displacement on the valley-side face, which was uncontrolled by geogrids, triggered the total collapse of the structure.

3 Numerical modelling

As previously mentioned, full-scale tests require large testing devices that are very expensive and difficult to manage. It is therefore necessary, at a design stage, to limit their number and to use their results to set up numerical models that are able to forecast the behaviour of the structure at various energy level impacts, as already done by

Table 3. Summary of the results of the full-scale tests.

| Test number | Impact energy [kJ] | Impact number | Mountain-side max displacement [m] | Valley-side max displacement [m] |
|-------------|--------------------|---------------|------------------------------------|----------------------------------|
| 1 | 2500 | 1 | 0.60 | 0.17 |
| | | 1 | 0.95 | 0.80 |
| 2 | 4500 | 2 | 1.30 | 1.20 |
| | | 3 | Collapse | – |
| 3 | 4500 | 1 | Collapse | – |

Carotti et al. (2000), Castiglia (2000), Di Prisco and Vecchiotti (2003, 2006), Bertrand et al. (2005), Bertrand (2006), Calvetti and Di Prisco (2007), Peila et al. (2007), Plassiard et al. (2008). These results, however, are mainly focused on a back-analysis of full-scale tests and do not provide a general overview of the embankment behaviour or design guidelines.

Reinforced embankments subjected to impact have therefore been studied using a systematic set of three-dimensional models developed with the ABAQUS/Explicit Finite Element Method code. The numerical algorithm on which the software is based is an explicit time integration known as “central difference method”. It is able to take into account the dynamic aspects of the problem, since the impact phenomenon lasts about 1 s with consequent large displacements in the structure. The computation is divided into several small time steps and the displacement, speed and acceleration of each node of the mesh are evaluated and registered at each time step.

The embankment soil was modelled with eight-node linear bricks using a Drucker-Prager yield criterion and a plastic hardening law. The soil was considered a homogeneous and mono-phase material and the presence of water was neglected. The geotechnical parameters (Table 4) were the usual ones of a granular soil used for embankment construction (Bowel, 1979; Lancellotta, 1995; Bourrier et

Table 4. Geotechnical parameters used for the embankment soil in the FEM numerical modelling.

| Geotechnical parameters for embankment soil | Values used in models |
|---|-----------------------|
| Mass density [kN/m ³] | 21 |
| Young's modulus [kPa] | 110 000 |
| Poisson's ratio [–] | 0.25 |
| Drained friction angle [°] | 34 |
| Drained cohesion [kPa] | 0 |
| Flow stress ratio [–] (ratio of the yield stress in triaxial tension to the yield stress in triaxial compression) | 0.78 |
| Dilatation angle [°] | 0 |
| Yield stress [kPa] | 540 |

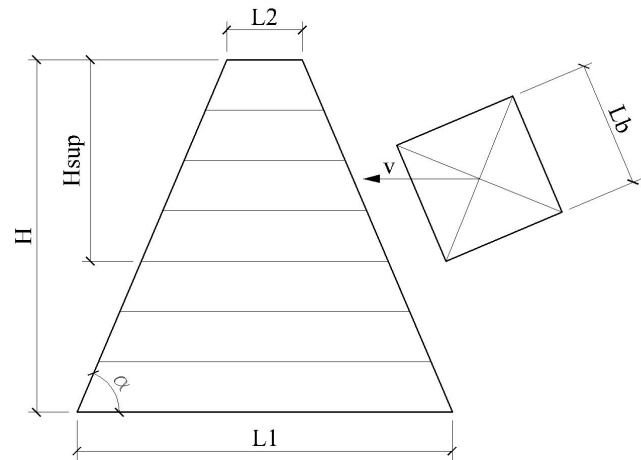
Table 5. Geometry parameters for the two modelled embankments (see Fig. 5 for symbols).

| Embankment type | L ₁ [m] | L ₂ [m] | V [m] | H [m] | H _{sup} [m] | α [°] |
|-----------------|--------------------|--------------------|-------|-------|----------------------|-------|
| 1 | 4.47 | 0.90 | 0.60 | 4.20 | 2.40 | 67 |
| 2 | 6.00 | 0.90 | 0.60 | 6 | 4.20 | 67 |

al., 2008). These data were used by Peila et al. (2007) for the back analysis of impact tests carried out on a reinforced embankment; the data were also derived from in situ tests carried out during the construction of the rockfall protection. The back analysis results showed good agreement between the measured data and the numerical results.

Due to numerical calculation problems linked to the management of the impact surfaces, the steel net was not modelled, although it is usually used in embankment faces. However, the full-scale tests have shown that this element is not significant as far as dynamic effects are concerned. The contact between the soil layers, which is obtained with the reinforcement elements, was modelled using a “master-slave weighted penalty method”, assuming a friction angle of 24° between the various layers. This is an average value which has been obtained from shear tests on geogrid elements (Del Greco and Oggeri, 1999). The adopted connection definition method checks for possible mesh collisions between the given surfaces or nodes during each time step and calculates the surface reaction force that is applied in the next time step. The impacting block was modelled as a perfectly rigid 1.5 m side body, with a friction angle of 22° between the block and the soil. This friction value was defined on the basis of the back analysis of some tamping tests (Mayne et al., 1994).

Two different sizes of the embankment (Table 5 and Fig. 5) were modelled to obtain results concerning rockfall protec-

**Fig. 5.** Geometry of the tested embankment and position of the impact. The nodes on the L₁ face are fixed. The soil layers can undergo horizontal and vertical displacements and deformations.

tion behaviour. In order to verify the reaction of the embankment at different energy levels and to obtain a design chart for the modelled structure, the speed of the impacting block was raised till the collapse energy was reached (constant block mass) for the different sizes of the embankment. Another series of models was developed by increasing the impacting block mass considering a constant impact velocity equal to 30 m/s. This last series was only developed for embankment type 2. A constant speed equal to 30 m/s was chosen since it seems to be the upper limit in rockfall events and because the negative dynamic effects are accentuated when this speed is assumed. Therefore, the obtained results can be presumed conservative as far as the design aspects are considered. The first series of analysis, conducted using various speeds, is instead useful to understand the effects of lower speed impacts.

The kinetic energy of the block, the energy dissipated in irreversible strains (plastic strain and friction), the acceleration, speed and displacement of the block and the shape of the deformed embankment were calculated for each simulation (Tables 6, 7 and 8 and Fig. 6).

The numerical results have confirmed that the layered structure influences the overall behaviour of the embankment, as only the layers directly involved in the impact exhibit important displacements (Fig. 7).

It was also possible to verify that 80÷85% of the kinetic energy of the block is used for soil compaction and plasticization of the impacted face, and therefore for the creation of the crater, while 15÷20% of the kinetic energy is dissipated by friction between the soil layers (Fig. 8 and Tables 6, 7 and 8). This last percentage increases from 15 to 20% with an increase in the impact energy level. The phenomenon can be explained considering that the energy which is dissipated in soil plasticization is reduced and a consequent increase in layers sliding occurs. These results are in agreement with

Table 6. Results obtained using the model of embankment 1 in the case of 1.50 m impacting block (see Fig. 6 for symbols). Key: E_{plast} : percentage of energy used for plastic deformation; E_{fric} : percentage of energy dissipated by friction between layers.

| E [kJ] | v [m/s] | ξ [m] | δ [m] | ψ [°] | E_{plast} [%] | E_{fric} [%] | Note |
|----------|-----------|-----------|--------------|------------|------------------------|-----------------------|----------|
| 1000 | 15.2 | 0.26 | 0.50 | 45 | 85 | 15 | – |
| 2000 | 21.4 | 0.50 | 0.90 | 40 | 85 | 15 | – |
| 4000 | 30.3 | 1.10 | 1.80 | 40 | 82 | 18 | collapse |

Table 7. Results obtained using the model of embankment 2 in the case of 1.50 m impacting block (see Fig. 6 for symbols). Key: E_{plast} : percentage of energy used for plastic deformation; E_{fric} : percentage of energy dissipated by friction between layers.

| E [kJ] | v [m/s] | ξ [m] | δ [m] | ψ [°] | E_{plast} [%] | E_{fric} [%] | Note |
|----------|-----------|-----------|--------------|------------|------------------------|-----------------------|----------|
| 1000 | 15.2 | 0.10 | 0.35 | 50 | 95 | 5 | – |
| 4000 | 30.3 | 0.30 | 0.95 | 50 | 85 | 15 | – |
| 6000 | 37.1 | 0.48 | 1.27 | 45 | 83 | 17 | – |
| 8000 | 42.9 | 0.72 | 1.60 | 45 | 83 | 17 | – |
| 10 000 | 47.9 | 0.90 | 1.90 | 40 | 82 | 18 | – |
| 12 000 | 52.5 | 1.10 | 2.30 | 40 | 82 | 18 | collapse |

Table 8. Results obtained using the model of embankment 2 in the case of constant impact velocity (equal to 30 m/s) and variable block mass (see Fig. 6 for symbols). Key: E_{plast} : percentage of energy used for plastic deformation; E_{fric} : percentage of energy dissipated by friction between layers.

| E [kJ] | m [kg] | ξ [m] | δ [m] | ψ [°] | E_{plast} [%] | E_{fric} [%] | Note |
|----------|----------|-----------|--------------|------------|------------------------|-----------------------|----------|
| 1125 | 2500 | 0.08 | 0.45 | – | 84 | 16 | – |
| 4500 | 10 000 | 0.42 | 0.87 | 55 | 85 | 15 | – |
| 6750 | 15 000 | 0.78 | 1.33 | 57 | 82 | 18 | – |
| 9000 | 20 000 | 1.45 | 1.99 | 54 | 79 | 21 | collapse |

those obtained by Peila et al. (2007), who developed a numerical back-analysis of the tests described in Chapter 2. The numerical models showed that the portion of the embankment involved in the impact is limited to a truncated cone shape (Fig. 9), which is in good agreement with the proposals given in OFROU Directive 12006 “Action de chutes de pierres sur les galeries de protection” (Frey, 1999).

If the displacements of both faces of the embankments are analyzed, with reference to the impact kinetic energy of the various models (Figs. 10, 11 and 12), it is possible to see that both displacement values grow with the impact energy with a linear trend until the collapse value is reached. These displacement values correspond to the minimum sliding-compaction of the embankment layers, therefore the centres of gravity of the layers involved in the impact and of the layers above are outside the bottom embankment support base. A 4.2 m high embankment impacted at a thickness of about 2.80 m with a 1.5 m boulder gives a collapse energy of 4000 kJ ($E_{\text{embankment}}$). Instead, if the height of the

embankment is raised to 6 m, with a thickness at the impact height of 4.50 m, the collapse energy is 12 000 kJ. In the case of the analysis with a constant impact block velocity value (assumed equal to 30 m/s) and variable block volumes, the 6 m high embankment impacted at a thickness of 4.50 m (as in case of the other models) collapsed with a 9000 kJ impact energy level (Fig. 12 and Table 8). This phenomenon highlights that the collapse energy decreases as the block sizes increase. Therefore, the embankment thickness at the impact height should be increased if the block sizes increase with the same energy level in order to maintain a certain safety factor.

The fact that the impact creates a crater on the embankment mountain-side face is why the rolling block does not pass the embankment. When a crater forms during impact, the rolling of the block mills the soil, thus dissipating high energy, and the block is stopped. This phenomenon has been verified using a numerical calculation in which a block is thrown against an embankment with a rotation speed of 20 rad/s (a very high value considering literature values)

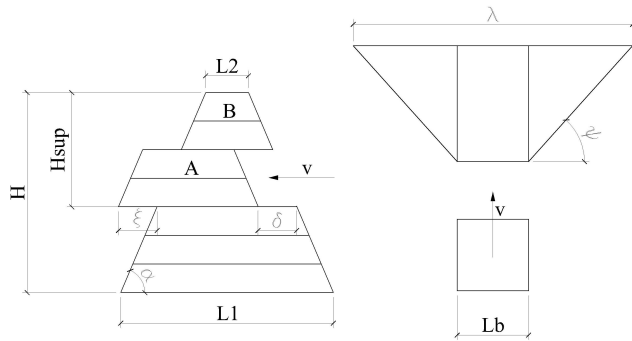


Fig. 6. Deformed shape of the theoretical reinforced embankment after the impact.

(Bourrier et al., 2009). The numerical results have confirmed that a rolling block is not able to excavate a trench on the mountain-side face and pass over the embankment. The only critical situation is when a block impacts on the top of the embankment, but this problem can be solved at the design level by introducing an adequate embankment height safety factor.

4 Design guidelines

Three-dimensional numerical models are usually difficult to calibrate in the dynamic field; a specialized engineer and a great deal of computational time are necessary. It cannot therefore be considered as a usual design tool and it would be useful to have a simplified analytical design approach that could permit a simple evaluation of a reinforced ground embankment to be used for rockfall protection (Peila and Oggeri, 2006). Other authors have introduced analytical approaches, based, for example, on force equilibrium taking into account the impact energy and the sharing energy on the subsoil by the moving ditch, which are useful to design both non-reinforced ditches and embankments reinforced with wood and steel bars (Tissieres, 1999).

For design purposes, apart from the static analysis of the embankment and the slope (bearing capacity of the foundations, sliding and tilting) and the internal stability of the embankment (tensile and pull-out strength of the reinforcing elements) (British Standard 8006), it is necessary to check that the structure can sustain the dynamic impact without launching fragments during the impact, without being passed over by rolling blocks and without collapsing due to block penetration and sliding of the soil layers.

The condition that the embankment should not launch rock fragments towards the valley during impact is always respected when reinforced soil is used, since the structure is made up of very small elements compared to the size of the falling block.

The risk of being passed over depends on the rolling speed of the falling block, but the block does not usually have

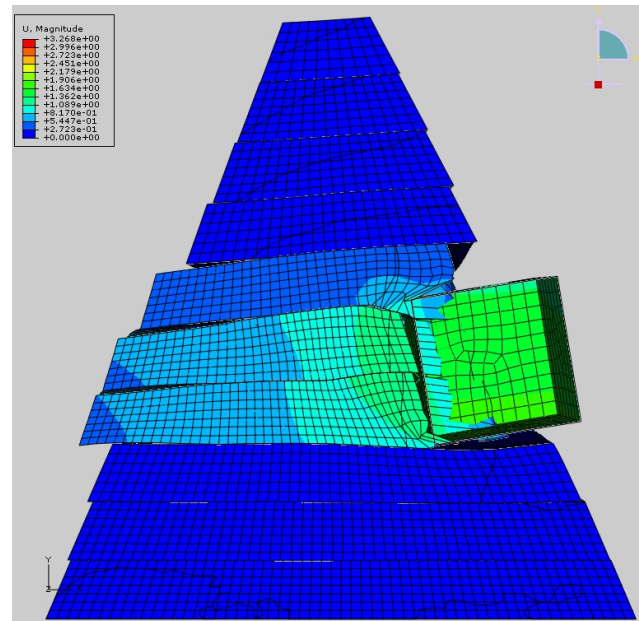


Fig. 7. Contour plot of the total displacements on impact with embankment 2, for an energy level of 6000 kJ. The sliding effect of the impacted layers is quite evident, while the remaining part of the embankment appears to be relatively undisturbed by the impact (at about 1 s after impact).

enough rotational energy to pass over the embankment after it has impacted and the crater has been created since the mountain-side face has a dip of about 70°.

A check on the stability of the structure during impact should involve verifying that the sliding of the soil layers involved in the impact and the plasticization of the soil on the mountain-side face, with the creation of the crater, do not trigger the global collapse of the embankment (Fig. 6). Therefore, the designer should check that:

a) the energy that can be sustained by the embankment ($E_{\text{embankment}}$) is greater than the energy of the falling block (E_{design}), which is linked to the size and speed of the falling block and which is computed using the classical physics formulations on the basis of the trajectory evaluation:

$$E_{\text{design}} - \frac{E_{\text{embankment}}}{\gamma_{ER}} \leq 0 \tag{1}$$

where γ_{ER} is the safety factor that has to be defined on the basis of the national regulations in force, for example using Eurocode 7 (EN 1997-1:2004), considering E_{design} as the action and $E_{\text{embankment}}$ as the resistance;

b) the interception height (h_i), that is, the embankment height minus the upper soil layer, is greater than the height of the computed trajectories of the falling block (h_{design}):

$$h_{\text{design}} - \frac{h_i}{\gamma_h} \leq 0 \tag{2}$$

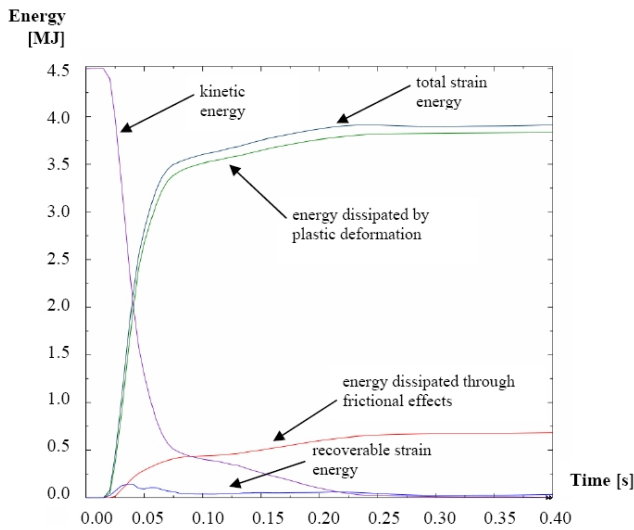


Fig. 8. Example of distribution of kinetic energy of the impacting block during the impact.

where γ_h is the safety factor that has to be defined on the basis of the national regulations in force, for example using Eurocode 7 (EN 1997-1:2004), considering h_{design} as the action and h_i as the resistance.

The energy that has to be sustained by the embankment ($E_{embankment}$) is computed by verifying the global stability of the structure after the impact, taking into account both the maximum sliding of the soil layers involved in the impact (ξ) and the plasticization of the soil with the penetration due to plasticization (δ_p). The total hole size on the mountain-side face is obtained adding δ_p to the sliding deformation component (ξ). All this is done considering the minimum size of a reinforced embankment with a certain height. If a thicker embankment is used, the global safety factor of the structure increases since the surfaces of the sliding layers increase up to a limit that corresponds to only the creation of the hole on the mountain-side face. This phenomenon can be understood from the collapse shown in Fig. 1, where the falling blocks are stopped and a hole is created but no movement can be observed on the valley-side face, and from the numerical calculation with impact energy equal to 1000 kJ (Table 7), where 95% of the energy is dissipated in plasticization phenomena.

The δ_p value can be obtained by evaluating the peak force that acts during the stopping phase (F_{max}) and by balancing 80÷85% of the kinetic energy of the block and the plastic deformation work done by the stopping force, which is assumed to have a triangular shape:

$$\delta_p = \frac{(0.80 \div 0.85) \cdot m v^2}{F_{max}} [m] \quad (3)$$

where: δ_p : the maximum penetration [m], m : the block mass [kg], v : the block velocity before the impact [m/s], F_{max} : the peak force during the stopping phase [N]. The choice

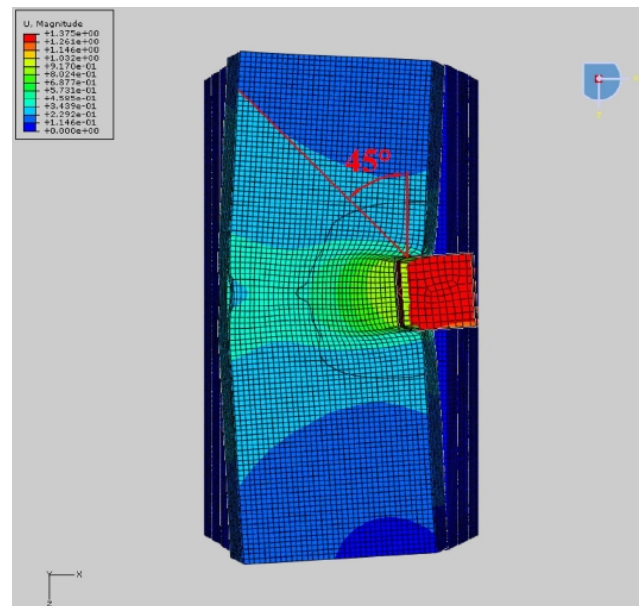


Fig. 9. Example of the contour plot of the displacements on impact with embankment 2 for an energy level of 4000 kJ. The truncated cone shape, which opened horizontally by an inclination angle γ of about 45° , is easily observable.

of the multiplicative coefficient derives from the energy impact level: 0.85 is chosen for an impact with less energy than 5000 kJ and 0.80 for an impact with more energy than 5000 kJ.

In order to compute F_{max} , it is possible to use the formula developed from the model proposed by Montani et al. (1996) and by Labiouse et al. (1996), which was derived from studies on rockfall shelter cover thickness:

$$F_{max} = 1.765 M_E^{2/5} R^{1/5} ((0.80 \div 0.85) E_{kin})^{3/5} [kN] \quad (4)$$

where: M_E : the cover soil elasticity coefficient (generally computed from the first load curve of a plate loading test) [kN/m²], R : the impacting block radius [m], E_{kin} : the block kinetic energy [kJ].

The ξ value can be computed by balancing 15÷20% of the kinetic energy of the block and the work absorbed by the friction forces (on the upper, lower and lateral sliding surfaces) due to the sliding of the layers as a rigid body. The choice of the multiplicative coefficient derives from the energy impact level: 0.15 is chosen for an impact with less energy than 5000 kJ and 0.20 for an impact with more energy than 5000 kJ. If the block sizes are of the same order of magnitude as the impacted embankment, only the lower and the lateral surfaces (and sometimes the base of the embankment) slide.

When ξ and δ_p are known, embankment design requires that the embankment, in the deformed shape, is stable after the impact. This condition can be verified through a static analysis of the deformed geometry stability, as shown

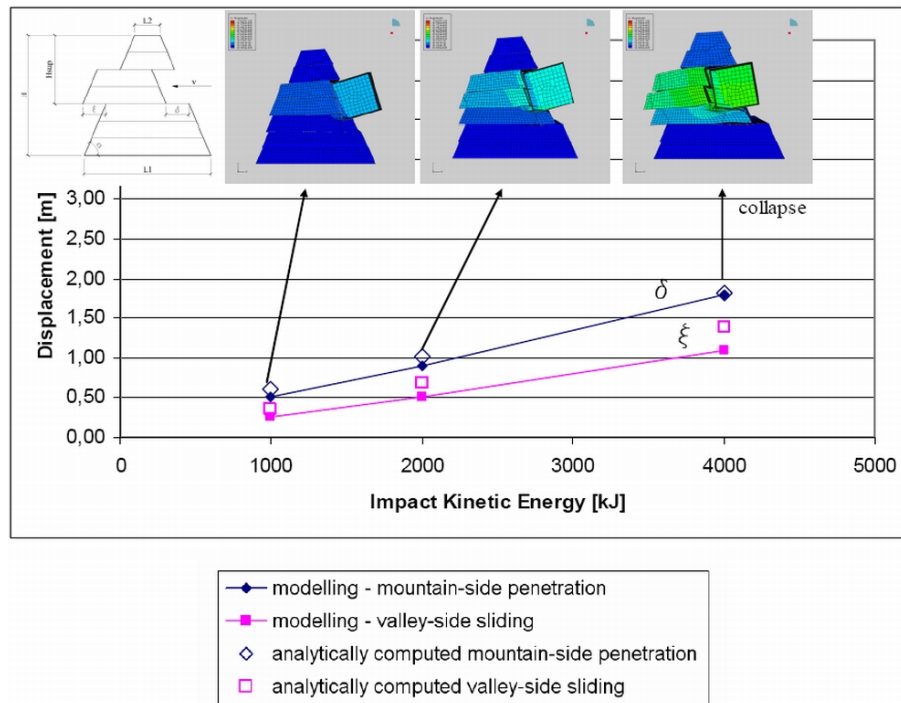


Fig. 10. Maximum displacements of both faces of embankment 1 in the case of 1.50 m impacting block evaluated using the numerical and analytical approaches, with reference to the impact kinetic energy. Key: the contour plot displacement varies from 0 m (deep blue colour) to 3.30 m (red colour).

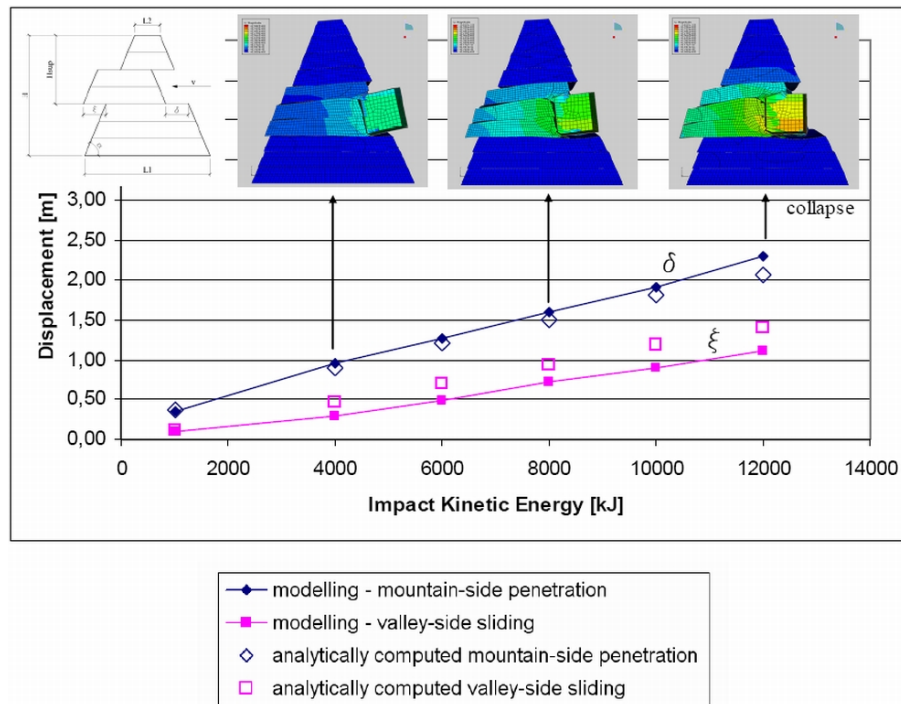


Fig. 11. Maximum displacements of both faces of embankment 2 in the case of 1.50 m impacting block evaluated using the numerical and analytical approaches, with reference to the impact kinetic energy. Key: the contour plot displacement varies from 0 m (deep blue colour) to 3.30 m (red colour).

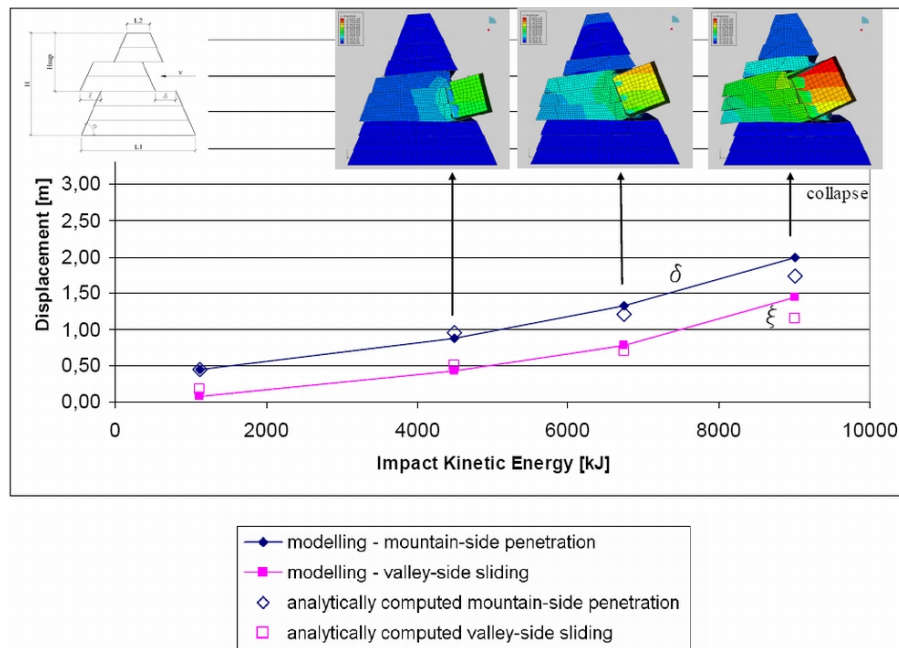


Fig. 12. Maximum displacements of both faces of embankment 2 evaluated using the numerical and analytical approaches, with reference to the impact kinetic energy, in the case of constant velocity, equal to 30 m/s. Key: the contour plot displacement varies from 0 m (deep blue colour) to 3.30 m (red colour).

in Fig. 6: the projection of centres of gravity of the impacted layers (elements named A) and of the layers above (elements named B) must be verified if they are outside the bottom embankment support base. The ψ value is derived from numerical modelling and is generally assumed equal to 45° .

In order to verify the quality of the proposed analytical approach, a comparison has been carried out between the numerical and analytical results (Figs. 10, 11 and 12). It has been found that they are in good agreement if an elasticity coefficient of the soil of 40 MPa (as proposed by Montani et al., 1996), a friction angle between the layers of 24° and ψ equal to 45° are considered. This analytical model could therefore be used for design purposes.

5 Conclusions

Reinforced embankments for rockfall passive protection can be considered a reliable solution because they permit both high energy levels and multiple impacts to be controlled. At the same time, these structures also lead to a reduction in maintenance activities for low energy impacts.

Full-scale tests carried out by different authors have demonstrated the feasibility of these structures, which obviously require larger spaces for their construction compared to net fences and also a careful preparation of a stable foundation ground.

Numerical modelling, developed on the basis of a back analysis of full-scale test results, can be used for design pur-

poses, but a numerical dynamic three-dimensional analysis is difficult to set up and requires long computational times. For this reason, a systematic modelling, that has been developed with blocks of different sizes impacting a geometrically standard reinforced embankment at different speeds and considering soil standard characteristics, has been developed and it has permitted a set of design charts to be obtained. Soil properties can be assessed by means of the tests usually carried out for road embankments, thus fulfilling the design requirements in terms of compaction, grain size distribution and deformability.

The literature on full-scale tests and numerical modelling have shown that a reinforced embankment, subjected to dynamic impacts of falling blocks, mainly deforms due to the sliding of the impacted layers and the plasticization of the impacted soil on the mountain-side face with the creation of a crater.

The numerical modelling has made it possible to observe that about 80–85% of the kinetic energy of a block is dissipated through soil compaction and plasticization, that is, with the creation of a crater, while only 15–20% is used to dislocate the impacted layers. If these two mechanisms of displacement are analyzed, it can be seen that both values grow linearly with the impact energy level. Furthermore, the volume that is deformed by the impact force does not involve the whole structure and only involves a trunk cone shaped section with an opening angle of about 45° , which starts at the crater boundary.

The deformed shape of the reinforced embankment after the impact can be schematized as a simple dislocation of the impacted layers and the collapse (that is, the ultimate limit state of the structure) is reached when the newly deformed shape is no longer statically stable. The computation has shown that a 4.20 m high reinforced embankment can absorb an impact of up to 4000 kJ with a maximum valley-side displacement of 1.10 m. A 6 m high embankment can instead safely absorb impacts of 12 000 kJ with a maximum displacement on the valley-side layers of 1.10 m. These results were obtained by modelling the impact of a 1.5 m cubic block with increasing speed and an impact height equal to 1.80 m. If the impacting speed is maintained at a constant value equal to 30 m/s and the block kinetic energy is raised by increasing the block size, it can be observed that the necessary collapse energy is reduced to 9000 kJ for a 6 m high reinforced embankment. This is probably due to the fact that there are more layers involved in the higher part of the embankment and therefore their confining action is reduced. It should be mentioned that some aspects have not been taken into account, namely uprolling, since the shape of the mountain-side face usually prevents this phenomenon, as demonstrated using a specific numerical computation. It should also be mentioned that it is possible to model multiple impacts at different heights using numerical modelling.

A new simplified analytical tool, where a work equilibrium analysis is carried out, has therefore been developed to evaluate the crater size on the mountain-side face and the layers sliding towards the valley-side face. This design scheme permits the deformed shape of the reinforced embankment subjected to block impact to be evaluated and its static stability to be estimated. The displacements obtained using this approach have been compared with FEM modelling results and a very good agreement has been observed.

The numerical approach is not simple to apply for a usual standard design, as it is necessary to model both the soil-reinforcing element interaction and the induced deformations over the whole structure. On the other hand, the proposed analytical approach is a practical design tool and its suitability has been demonstrated through a comparison with the site tests and the numerical modelling results.

The choice of an embankment can be based both on design charts developed using numerical modelling or the proposed analytical approach. However it should be recalled that the local and global stability of the slope where the embankment is built, the embankment drainage attitude with reference to the slope surface hydrology and the properties and heterogeneity of the adopted soil are also essential elements for a complete design.

Acknowledgements. This study was financially supported by both the Officine Maccaferri S.p.A., as part of a research project with the Politecnico di Torino, and by a National Research Project of Italian Ministry of University and Research (PRIN 2007 – Application of advanced technologies to the safety, environmental protection,

optimization of management and yield in quarry: geomining characterization and monitoring methodologies – National coordinator: P. Berry; Research unit of DITAG, Politecnico di Torino, Local coordinator: D. Peila).

The authors have contributed to the development of this paper to the same extent.

Edited by: A. Volkwein

Reviewed by: two anonymous referees

References

- Barrett, R. K. and White, J. L.: Rock fall prediction and control, in: Proceedings of National Symposium on Highway and Railway Slope Maintenance, Association of Engineering Geologists, Chicago, USA, 23–40, 1991.
- Bertrand, D.: Modélisation du comportement mécanique d'une structure cellulaire soumise à une sollicitation dynamique localisée, Ph.D. thesis, Université Joseph Fourier, Grenoble, France, 2006.
- Bertrand, D., Nicot, F., Gotteland, P., and Lambert, S.: Modelling a geo-composite cell using discrete analysis, *Comput. Geotech.*, 32(8), 564–577, 2005.
- Bourreir, F., Dorren, L., Nicot, F., Berger, F., and Darve, F.: Toward objective rockfall trajectory simulation using a stochastic impact model, *Geomorphology*, in press, 2009.
- Bourrier, F., Nicot, F., and Darve, F.: Physical processes within a 2-D granular layer during an impact, *Granul. Matter*, 10(6), 415–437, 2008.
- Bowel, J. E.: Physical & geotechnical properties of soils, McGraw Hill Book Co., Auckland, New Zealand, 478 pp., 1979.
- British Standard 8006: Code of practice: strengthened reinforced soils and other fills, 1995.
- Burroughs, D. K., Henson, H. H., and Jiang, S. S.: Full scale geotextile rock barrier wall testing, analysis and prediction, in: Proceedings of Geosynthetics 1993, Vancouver, Canada, 30 March–1 April 1993, 959–970, 1993.
- Calvetti, F. and Di Prisco, C.: Linee guida per la progettazione di gallerie paramassi, Starrylink Editrice Brescia, Brescia, Italy, 184 pp., 2007.
- Carotti, A., Peila, D., Castiglia, C., and Rimoldi, P.: Mathematical modelling of geogrid reinforced embankments subject to high energy rock impact, in: Proceedings of Eurogeo, II European Geosynthetics Conference and Exhibition, Bologna, Italy, 15–18 October 2000, 305–310, 2000.
- Castiglia, C.: Studio del comportamento di rilevati paramassi, M.S. thesis, Politecnico di Torino, Italy, 2000.
- Del Greco, O., Fornaro, M., and Oggeri, C.: Modification of a quarry face: stabilization criteria and environment reclamation, in: Proceedings of 7th International Congress IAEG, Lisboa, Portugal, 5–9 September 1994, 4109–4118, 1994.
- Del Greco, O. and Oggeri, C.: Caratteristiche di resistenza a taglio di geosintetici, in: Proceedings of XX Convegno Nazionale di Geotecnica, Parma, Italy, 22–25 September 1999, 79–86, 1999.
- Di Prisco, C. and Vecchiotti, M.: Impatti di blocchi di roccia su rilevati rinforzati: modellazione teorica e spunti progettuali, *L'Ingegnere e l'Architetto*, 10(1), 62–69, 2003.

- Di Prisco, C. and Vecchiotti, M.: A rheological model for the description of boulder impacts on granular strata, *Geotechnique*, 56(7), 469–482, 2006.
- EN 1997-1: Eurocode – Geotechnical design – Part 1: General rules, 168 pp., 2004.
- Frey, R. P.: Swiss guideline: action on rockfall protection galleries, in: *Proceedings of the Joint Japan-Swiss Scientific Seminar on Impact load by rock fall and design of protection structures*, Kanazawa, Japan, 4–7 October 1999, 91–94, 1999.
- Giani, G. P.: *Rock slopes stability analysis*, Balkema, Rotterdam, Netherlands, 347 pp., 1992.
- Labieuse, V., Descoedres, F., and Montani, S.: Experimental study of rock sheds impacted by rock blocks, *Structural Engineering International*, 3, 171–175, 1996.
- Lambert, S., Gotteland, P., Bertrand, D., and Nicot, F.: Comportement mécanique de géo-cellules soumises à impact, in: *Proceedings of Congr s de M canique*, Grenoble, France, 27–31 August 2007, 23–24, 2007.
- Lambert, S., Nicot, F., and Gotteland, P.: Experimental study of the impact response of geo-cells as components of rockfall protections diches, in: *Proceedings of Interdisciplinary Workshop on Rockfall Protection*, Morschach, Switzerland, 23–25 June 2008, 52–54, 2008.
- Lancellotta, R.: *Geotechnical Engineering*, Balkema, Rotterdam, Netherlands, 436 pp., 1995.
- Lazzari, A., Troisi, C., and Arcuri, G.: Protezione di nuclei abitati contro la caduta di massi mediante rilevati in terra rinforzata: esperienze della Regione Piemonte, in: *Proceedings of Giornata di Studio su La protezione contro la caduta di massi dai versanti rocciosi*, Torino, Italy, 24 October 1996, 85–94, 1996.
- Mayne, P. W., Jones, J. J., and Dumas, J. C.: Ground response to dynamic compaction, *J. Geotech. Eng.-ASCE*, 110(6), 757–774, 1994.
- Montani, S., Descoedres, F., and Egger, P.: Impact de blocs rocheux sur des galeries de protection, in: *Proceedings of Giornata di Studio “La protezione contro la caduta massi dai versanti rocciosi”*, Torino, Italy, 24 October 1996, 55–64, 1996.
- Nomura, T., Inoue, S., Fuchigami, M., Yokota, Y., Kubo, T., Tatta, N., and Arai, K.: Experimental research of reinforced soil wall for rock-fall protection, in: *Proceedings of 7th International conference on geosynthetics*, Nice, France, 22–27 September, 303–308, 2002.
- OFROU Directive 12006: Action de chutes de pierres sur les galeries de protection, www.astra.admin.ch, access: 30 January 2009, v. 2.03, 2008.
- Oggeri, C. and Peila, D.: Protection of transportation system against rock falls, in: *Proceedings of Landslides in research, theory and practice*, 8th International Symposium on Landslides, Cardiff, UK, 26–30 June 2000, 1141–1146, 2000.
- Oggeri, C., Peila, D., and Recalcati, P.: Rilevati paramassi, in: *Proceedings of Convegno Bonifica di versanti rocciosi per la protezione del territorio*, Trento, Italy, 11–12 March 2004, 191–232, 2004.
- Paronuzzi, P.: Criteri di progettazione di rilevati paramassi, *Geologia tecnica*, 1, 23–41, 1989.
- Pasqualotto, M., Hugonin, B., and Vagliasindi, B.: Rilevati in terra rinforzata a protezione dalla caduta massi in Val di Rhemes (AO), *GEAM Geoingegneria Ambientale e Mineraria*, 114(1), 55–67, 2005.
- Pasqualotto, M., Peila, D., and Oggeri, C.: Prestazioni di un sistema di rilevati a scogliera soggetti ad impatto di massi, in: *Proceedings of Convegno Bonifica di versanti rocciosi per la protezione del territorio*, Trento, Italy, 11–12 March 2004, 435–442, 2004.
- Peckover, F. L. and Kerr, W. G.: Treatment and maintenance of rock slopes on transportation routes, *Can. Geotech. J.*, 14(4), 487–507, 1977.
- Peila, D., Castiglia, C., Oggeri, C., Guasti, G., Recalcati, P., and Sassudelli, F.: Full scale tests on geogrid reinforced embankments for rock fall protection, in: *Proceedings of 2nd European Geosynthetics Conference and Exhibition*, Bologna, Italy, 15–18 October 2000, 317–322, 2000.
- Peila, D. and Oggeri, C.: Tecnologia e aspetti progettuali di interventi di bonifica e di messa in sicurezza di versanti rocciosi soggetti a fenomeni di caduta massi, in: *Proceedings of XI Ciclo di Conferenze di Meccanica e Ingegneria delle Rocce*, Torino, Italy, 28–29 November 2006, 85–112, 2006.
- Peila, D., Oggeri, C., and Castiglia, C.: Ground reinforced embankments for rockfall protection: design and evaluation of full scale tests, *Landslides Investigations and Mitigation*, 4(3), 255–265, 2007.
- Peila, D., Oggeri, C., Castiglia, C., Recalcati, P., and Rimoldi, P.: Testing and modelling geogrid reinforced soil embankments to high energy rock impacts, in: *Proceedings of 7th I.C.G.*, Nice, France, 22–27 September 2002, 133–136, 2002.
- Peila, D., Pelizza, S., and Sassudelli, F.: Evaluation of behaviour of rockfall restraining nets by full scale tests, *Rock Mech. Rock Eng.*, 31(1), 1–24, 1998.
- Peila, D., Rimoldi, P., Recalcati, P., Guasti, G., and Castiglia, C.: Prove in vera grandezza su rilevati paramassi rinforzati con geogriglie, *GEAM Geoingegneria Ambientale e Mineraria*, XXXVI(2–3), 149–154, 1999.
- Plassiard, J. P., Donz , F. V., and Lorentz, J.: Simulations of rockfall impacts on embankments using a discrete element method, in: *Proceedings of Interdisciplinary Workshop on Rockfall Protection*, Morschach, Switzerland, 23–25 June 2008, 84–86, 2008.
- Protec Engineering: <http://www.proteng.co.jp>, access: 30 January 2009.
- Tissieres, P.: Ditches and reinforced ditches against falling rocks, in: *Proceedings of the Joint Japan-Swiss Scientific Seminar on Impact load by rock fall and design of protection structures*, Kanazawa, Japan, 4–7 October 1999, 65–68, 1999.
- Wyllie, C. W. and Norrish, I. N.: *Stabilization of rock slopes*, *Landslides Investigations and Mitigation*, 247, 474–506, 1996.
- Yoshida, H.: Recent experimental studies on rockfall control in Japan, in: *Proceedings of the Joint Japan-Swiss Scientific Seminar on Impact load by rock fall and design of protection structures*, Kanazawa, Japan, 4–7 October 1999, 69–78, 1999.